Exacerbation of collagen type II-induced arthritis in ApoE deficient mice in association with the expansion of Th1 and Th17 cells.

Jorge Postigo, BS[1], Fernanda Genre, BS[1], Marcos Iglesias, BS[1,2], Maigualida Fernández-Rey, BS[1], Luis Buelta, MD, PhD[3], José Carlos Rodríguez-Rey, PhD[1], Jesús Merino, MD, PhD[1] and Ramón Merino, MD, PhD[2]

[1]Departamento de Biología Molecular, Universidad de Cantabria-IFIMAV, [2]Instituto de Biomedicina y Biotecnología de Cantabria/CSIC-Universidad de Cantabria-SODERCAN and [3]Departamento de Ciencias Médicas y Quirúrgicas, Universidad de Cantabria, Santander, Spain.

Correspondence: Dr. Ramón Merino, IBBTEC, Departamento de Biología Molecular, Facultad de Medicina, Cardenal Herrera Oria s/n, 39011 Santander, Spain.

Phone: 4 942 201956

Fax: 34 942 201945

e-mail: merinor@unican.es

Running head: ApoE deficiency exacerbates CIA

This work was supported by grants from the Ministerio de Educación y Ciencia, Spain to RM (SAF2008-02042) and JM (BFU2009-07206) and from Fundación Eugenio Rodríguez Pascual, Spain to RM. FG is supported by a pre-doctoral fellowship from the Instituto Danone, Spain.

ABSTRACT

Objective. To explore the bidirectional relationship between the development of rheumatoid arthritis and atherosclerosis using bovine collagen type II (col II) immunized B10.RIII.ApoE$^{-/-}$ mice, a murine model of spontaneous atherosclerosis and collagen-induced arthritis (CIA).

Methods. B10.RIII.ApoE$^{-/-}$ male mice and wild type controls were immunized with 150 μg of col II emulsified in complete Freund's adjuvant (CFA). The clinical, radiological and histopathological severity of CIA, the levels of circulating IgG1 and IgG2a anti-col II antibodies, the expression of pro- and anti-inflammatory cytokines in the joints and the percentages of Th1, Th17 and Treg lymphocytes in the draining lymph nodes were evaluated during CIA induction. In addition, the size of atherosclerotic lesions was assessed in these mice 8 weeks after CIA induction.

Results. Col II-CFA immunized B10.RIII.*ApoE*$^{-/-}$ mice developed an exacerbated CIA that was accompanied by increased joint expression of multiple pro-inflammatory cytokines and by the expansion in the draining lymph nodes of Th1 and Th17 cells. In contrast, the size of vascular lesions in B10.RIII.*ApoE*$^{-/-}$ mice was not affected by the development of CIA.

Conclusions. We demonstrate here that the deficiency in ApoE and/or its consequences in cholesterol metabolism act as accelerating factors in autoimmunity by promoting Th1 and Th17 inflammatory responses.

INTRODUCTION

Rheumatoid arthritis (RA), a chronic autoimmune disease resulting in joint inflammation and destruction, is associated with an increased risk of cardiovascular (CV) disease due to accelerated atherosclerosis (1, 2). The inflammatory environment associated to RA, rather than traditional CV risk factors, has been postulated to be implicated in the accelerated atherosclerosis of these patients (3). In addition, an association between active RA and altered lipid profiles in plasma, manifested by low high-density lipoprotein-cholesterol (HDLc) levels, high total cholesterol/HDLc ratio and high triglyceride levels, has been established (4-6). These unfavorable lipid changes may already be present at least 10 years before the onset of RA (7), suggesting their potential involvement in the initiation and/or activity of this systemic autoimmune disease. In fact, HDL not only participates in the reverse transport of cholesterol, promoting cellular cholesterol efflux from peripheral cells to the liver for excretion, but also possesses anti-inflammatory properties, including its ability to protect low-density lipoprotein (LDL) from oxidation (8-11). However, the mechanistical relationship between altered plasma lipid profiles and active RA lacks of appropriate experimental evidences in well defined animal models.

Mice deficient in ApoE (*ApoE*$^{-/-}$) constitute an excellent animal model to explore metabolic and immunological mechanisms involved in atherosclerosis (12, 13). These mice spontaneously develop atherosclerosis in a time and diet dependent manner in association with reduced HDLc and increased total cholesterol and LDL-cholesterol (LDLc) levels in plasma. On the other hand, immunization of susceptible strains of mice, such as B10.RIII (H-2^{r}) mice, with bovine collagen type II (col II) emulsified in complete Freund's adjuvant (CFA) develop a destructive joint inflammatory disease resembling human RA (14). Both atherosclerosis in *ApoE*$^{-/-}$ mice and col II-induced

arthritis (CIA) in predisposed animals are mediated by a particular functional subpopulation of antigen-driven $CD4^+$ cells, termed Th17 cells, producing IL-6, IL-17A and IL-21 cytokines (15-19). In fact, blockade of IL-17A results in reduced atherosclerosis in *ApoE*$^{-/-}$ mice and animals with an impaired Th17 differentiation develop an attenuated form of CIA (13, 17, 18). Using B10.RIII.*ApoE*$^{-/-}$ mice immunized with bovine col II-CFA, here we investigated whether the pro-inflammatory and/or metabolic alterations that have been involved in the pathogenesis of each process separately, collaborate in promoting an accelerated atherosclerosis and/or arthritis. Unlike a recent study in C56BL/6.*ApoE*$^{-/-}$ (B6.*ApoE*$^{-/-}$) mice immunized with chicken col II-CFA (20), our results demonstrate that B10.RIII.*ApoE*$^{-/-}$ mice develop an accelerated and exacerbated CIA after immunization with col II-CFA. This enhanced severity is accompanied by an increased expression of multiple pro-inflammatory cytokines in the joints and by the expansion of Th1 and Th17 cells in the draining lymph nodes. In contrast, the intensity of vascular lesions in col II-CFA immunized B10.RIII.*ApoE*$^{-/-}$ mice is not affected by the development of CIA.

MATERIAL AND METHODS

Mice.

B6.*ApoE*$^{-/-}$ (H-2^b) and B10.RIII (H-2^r) mice were purchased from Charles River (Barcelona, Spain) and Harlan Iberica (Barcelona, Spain), respectively. B10.RIII.*ApoE*$^{-/-}$ mice were obtained in our animal facilities by backcrossing B6.*ApoE*$^{-/-}$ mice with B10.RIII mice for 10 generations. At the second backcross generation, H-$2^{r/r}$ mice were selected by flow cytometry using specific mAbs against H-2^b and H-2^r (BD Biosciences, Madrid, Spain). At the 10^{th} backcross generation, male and female B10.RIII.*ApoE*$^{+/-}$ mice were intercrossed and the resulting *ApoE*$^{-/-}$ homozygous mice were selected by

PCR of genomic DNA extracted from mouse tails. Mice were fed ad libitum with a normal chow diet and bled from the retro-orbital plexus 8 weeks after immunization.

All studies with live animals were approved by the Universidad de Cantabria Institutional Laboratory Animal Care and Use Committee.

Induction and assessment of arthritis.

Bovine col II (provided by Dr Marie Griffiths, University of Utah) was dissolved at a concentration of 2 mg/ml in 0.05 M acetic acid and emulsified with CFA containing 4 mg/ml of *Mycobacterium tuberculosis* (MD Bioproducts, Zürich, Switzerland). For the induction of CIA, 8-12 weeks-old male mice were immunized once at the base of the tail with 150 μg of antigen in a final volume of 150 μl. In some experiments, mice receiving an injection of PBS-CFA were used as CIA negative controls. A clinical evaluation of arthritis severity was performed as described (21).

Radiological studies were performed using a CCX Rx ray source of 70 Kw with an exposition of 90 ms (Trophy Irix X-Ray System; Kodak Spain, Madrid) and Trophy RVG Digital Imagining system, as previously described (21). Radiological images were scale graded according to the presence of 4 different radiological lesions (1: soft tissue swelling, 2: juxtaarticular osteopenia due to alterations in bone density, 3: joint space narrowing or disappearance and 4: bone surface irregularities due to marginal erosions and/or periosteal new bone formation). The extension of every individual lesion in each paw (local: affecting one digit or one joint in the carpus; diffuse: affecting two or more digits and/or two or more joints in the carpus) was graded from 0 to 2 as follow: 0: absence; 1: local; 2: diffuse.

Mice were killed 8 weeks after immunization and the hind paws were fixed in 10% phosphate-buffered formaldehyde solution and decalcified in Parengy's

decalcification solution overnight. The tissue was then embedded in paraffin. Sections (5 μm) were stained with hematoxylin and eosin, examined in a light-phase microscope and scored according to a 0 to 3 scale as described previously (22).

Serological studies.

Total cholesterol, HDL-c, LDL/VLDL-c and triglyceride levels in serum samples were determined using enzymatic assays (cholesterol assay kit, BioVision, Inc., Mountain View, CA and Triglyceride-LQ assay, Spinreact, Girona, Spain) following the manufacturer instructions. Serum levels of IgG1 and IgG2a anti-col II antibodies were measured by ELISA as described (23). Results were expressed in TU in reference to a standard curve obtained from a serum pool from col II-CFA immunized DBA/1 mice. Serum levels of total IgG1 and IgG2a were determined by ELISA as described (24). Results were expressed in mg/ml in reference to a standard curve obtained with a mouse reference serum (MP Biomedicals, Irvine, CA).

Flow cytometry studies.

The percentages of Th1and Th17 in the draining lymph nodes of B10.RIII.WT and B10.RIII.*ApoE*$^{-/-}$ mice before and 3 weeks after immunization with col II-CFA were determined by flow cytometry. Intracellular cytokine staining was performed using an intracellular staining kit (BD Biosciences). Lymphocytes from paraaortic lymph nodes were stimulated with phorbol myristate acetate (50 ng/ml) and ionomycin (750 ng/ml) in the presence of GolgiStop solution (BD Biosciences) for 6 hours and stained with fluorescein isothiocyanate–conjugated anti-CD4 and phycoerythrin-conjugated anti-IFNγ or phycoerythrin-conjugated anti–IL-17 (all antibodies from BD Biosciences). A phycoerythrin-conjugated IgG2a irrelevant antibody was used as an isotype control of

cytokine staining. The percentages of $CD4^+CD25^+FoxP3^+$ regulatory T cells (Tregs) were determined at the same time points by flow cytometry using conjugated mAbs, as described previously (21). A total of 5×10^4 viable cells were analyzed in a FACSCanto II flow cytometer using FACSDiva software (BD Biosciences).

Quantitative real-time RT-PCR analyses.

Total RNA was obtained from joints by TRIzol extraction (Invitrogen, Life Technologies Corporation, Carlsbad, CA). One μg of the isolated RNA was used for cDNA synthesis with a RT-PCR kit (Amersham Pharmacia Biotech, Piscataway, NJ), according to the manufacturer instructions. Quantitative real time RT-PCR was performed on a MX-3000P Stratagene instrument (Agilent Technologies, Inc., Santa Clara, CA) using specific TaqMan expression assays and universal PCR Master Mix (Applied Biosystems, Life Technologies Corporation). Results (in triplicate) were normalized to *GAPDH* expression and measured in parallel in each sample. Data were expressed as mean fold change relative to control samples.

Evaluation of atherosclerosis.

The extension of atherosclerosis was quantified as previously described (25). Briefly, 8-10 sections (5 μm) at 50-μm intervals from paraffin-embedded aortic sinus of PBS-CFA immunized and col II-CFA immunized B10.RIII.*ApoE*$^{-/-}$ mice were stained with hematoxylin and eosin. Lesion size was determined by computer-assisted morphometry and expressed as the percentage of the surface area of the aorta occupied by lesions according to the following formula: [Σ Area of Lesion/Σ Total Internal Perimeter of the Aorta)]×100. For cellular characterization of atherosclerotic lesions, macrophages were detected by immunohistochemistry with a biotin-labelled rat anti-

Mac2 monoclonal antibody (clone M3/38, Cedarlane Laboratories, Hornby, ON, Canada), followed by streptavidin-HRP (BD Biosciences), and DAB substrate (Dako Diagnósticos, S.A., Barcelona Spain). Specimens were counterstained with hematoxylin. Staining with anti-Mac2 was expressed as percentage of stained surface area within the lesions (anti-Mac2-stained surface/total lesion surface x 100), as described (26).

Statistical analysis.

Statistical analysis of differences between groups of mice was performed using the Mann-Whitney test. Probability values <0.05 were considered significant.

RESULTS

Development of a severe CIA in B10.RIII.*ApoE*$^{-/-}$ mice.

To explore whether the deficiency in ApoE influenced the clinical progression of CIA in B10.RIII mice, we immunized B10.RIII wild type (WT) and B10.RIII.*ApoE*$^{-/-}$ mice with col II-CFA. We first analyzed serum lipid profiles in these groups of mice 8 weeks after immunization. As expected (13), immunized B10.RIII.*ApoE*$^{-/-}$ mice presented circulating levels of total cholesterol and triglycerides higher than B10.RIII.WT mice ($p<0.001$) (Figure 1A and 1B). The elevated cholesterol levels in these mice was basically due to the increase in the LDL/VLDL-c fraction since the levels of serum HDL-c were essentially identical in both groups of mice (Figure 1). The circulating lipid profiles detected in B10.RIII.WT and B10.RIII.*ApoE*$^{-/-}$ mice 8 weeks after immunization with col II-CFA were similar to those observed before immunization (data not shown). Based on these results and to avoid additional metabolic alterations introduced by hypercholesterolemic diets, we decided to perform all the experiments in mice fed with a normal chow diet.

We next compared the development of CIA between B10.RIII.WT and B10.RIII.*ApoE*$^{-/-}$ mice. Unlike previous reports (20), B10.RIII.*ApoE*$^{-/-}$ mice developed a more accelerated CIA than B10.RIII.WT mice and exhibited an increased cumulative incidence throughout the 8 week period of survey (Figure 2A). In addition, the clinical severity of CIA 8 weeks after col II-CFA immunization was also significantly higher in B10.RIII.*ApoE*$^{-/-}$ than in B10.RIII.WT mice (Figure 2B). In correlation with the clinical findings, the severity of every individual radiological sign considered here (soft tissue swelling, juxtaarticular osteopenia, narrowing or disappearance of the interosseous spaces reflecting cartilage loss and bone irregularities secondary to periosteal new bone formation and/or marginal articular erosions) was significantly higher in B10.RIII.*ApoE*$^{-/-}$ than in B10.RIII.WT mice (Figure 3A and B). By histological analyses, the joints from B10.RIII.*ApoE*$^{-/-}$ mice more frequently showed signs of severe autoimmune arthritis such as widespread infiltration of inflammatory cells, pannus formation, cartilage destruction and bone erosion (Figure 3C and D).

Altered anti-col II antibody production in B10.RIII.*ApoE*$^{-/-}$ mice.

The intensity and quality of anti-col II humoral immune responses was compared between B10.RIII.WT and B10.RIII.*ApoE*$^{-/-}$ mice by analyzing the levels of circulating IgG1 and IgG2a anti-col II antibodies. Both groups of mice exhibited strong anti-col II antibody responses 8 weeks after CIA-induction (Figure 2C). However, qualitative differences in these antibody responses were observed between B10.RIII.WT and B10.RIII.*ApoE*$^{-/-}$ mice. Thus, whereas serum levels of IgG2a anti-col II antibodies were similar in both groups of mice, the titres of IgG1 anti-col II antibodies were significantly reduced in B10.RIII.*ApoE*$^{-/-}$ mice (Figure 2C). The altered anti-col II humoral immune response was antigen specific since the levels of circulating total IgG1

and IgG2a antibodies 8 weeks after CIA-induction were similar in B10.RIII.WT and B10.RIII.*ApoE*$^{-/-}$ mice (serum levels of total IgG1 antibodies in B10.RIII.WT mice: 0.9 ± 0.4 mg/ml; in B10.RIII.*ApoE*$^{-/-}$ mice: 1.1 ± 0.3 mg/ml; serum levels of total IgG2a antibodies in B10.RIII.WT mice: 3.6 ± 1.1 mg/ml; in B10.RIII.*ApoE*$^{-/-}$ mice: 3.1 ± 1.7 mg/ml; $p > 0.5$ in both cases).

Increased joint expression of pro-inflammatory cytokines and expansion of Th1 and Th17 cells in B10.RIII.*ApoE*$^{-/-}$ mice.

The exacerbated development of CIA in B10.RIII.*ApoE*$^{-/-}$ mice together with the reduction in the levels of circulating IgG1 anti-col II antibodies compared to B10.RIII.WT mice, prompted us to explore by quantitative real time RT-PCR the pattern of cytokine expression in the joints during the induction of CIA in these strains of mice. As expected (27), a significant increase in the expression of the arthritogenic IL-1β, TNFα and IL-6 transcripts was observed in the joints of B10.RIII.WT mice 8 weeks after immunization with col II-CFA (Figure 4). In addition, joint levels of IFNγ and IL-17 mRNAs but not of TGFβ1, IL-4 and IL-21 mRNAs were augmented in B10.RIII.WT mice with arthritis (Figure 4). In parallel with the aggravated CIA, the expression of IL-1β, IL-6, IFNγ, IL-17 and IL-21 transcripts, but not of TNFα, TGFβ1 and IL-4, in the joints of col II-immunized B10.RIII.*ApoE*$^{-/-}$ mice was even higher than that found in CIA-developing B10.RIII.WT mice (Figure 4).

Due to the pattern of cytokine expression in the joints and to further explore the mechanisms implicated in the worsening of CIA in B10.RIII.ApoE$^{-/-}$ mice, we compared the percentages of different functional CD4^{+} T-cell subpopulations in the draining lymph nodes of B10.RIII.WT and B10.RIII.*ApoE*$^{-/-}$ mice before and after immunization with col II-CFA. Both IFNγ-producing Th1 and IL-17-producing Th17

cell populations were augmented in the paraaortic lymph nodes from B10.RIII.WT mice 3 weeks after immunization with col II-CFA (Figure 5). Again, this increase was significantly higher (about two fold) in B10.RIII.*ApoE*$^{-/-}$ mice (Figure 5). No differences in the percentage of Tregs were observed between non-immunized and immunized B10.RIII.WT and B10.RIII.*ApoE*$^{-/-}$ mice (Figure 5).

Lack of exacerbation of atherosclerosis in CIA-developing B10.RIII.*ApoE*$^{-/-}$ mice.

We next investigated whether the development of a severe CIA in B10.RIII.*ApoE*$^{-/-}$ mice might in turn modify the clinical evolution of atherosclerosis in these mutant mice. Since adjuvants, including CFA, have potent atheromodulating capabilities in *ApoE*$^{-/-}$ mice (25), we used B10.RIII.*ApoE*$^{-/-}$ mice receiving only PBS emulsified in CFA at the base of the tail as the CIA negative controls of this experiment, and as expected, these mice failed to develop arthritis (data not shown). Morphometric studies in the aortic sinus 8 weeks after immunization revealed that the extent of atherosclerotic area in col II-CFA immunized B10.RIII.*ApoE*$^{-/-}$ mice was similar to that of PBS-CFA treated B10.RIII.*ApoE*$^{-/-}$ controls (Figures 6A and 6B; $p>0.6$). In addition, a similar content of Mac2-immunoreactive macrophages was observed by immunohistochemistry in the atherosclerotic lesions of PBS-CFA treated and col II-CFA immunized B10.RIII.*ApoE*$^{-/-}$mice (Figures 6A and 6C; $p>0.5$).

DISCUSSION

In the present study we have explored the bidirectional relationship between RA and atherosclerosis development using an experimental model in mice. We demonstrate here that the deficiency in ApoE and/or its consequences in cholesterol metabolism promote an accelerated and aggravated form of CIA in predisposed B10.RIII mice. The

exacerbated CIA is accompanied by an increased joint expression of multiple pro-inflammatory cytokines and by the expansion in the draining lymph nodes of Th1 and Th17 cell populations. On the other hand, the evolution of atherosclerosis in these B10.RIII.*ApoE*$^{-/-}$ mice seems to be unchanged by the development of CIA. Our results clearly contrast with a recent report showing a resistance to CIA development in ApoE deficient mice (20). Although the reasons for these discrepancies are not clear, they can be related to the different CIA models used in both studies that may involve immunological mechanisms that do not completely overlap. Thus, whereas we have used H-2^{r} CIA-susceptible B10.RIII mice immunized with bovine col II, the other study has been performed in B6 (H-2^{b}) mice immunized with chicken col II in which CIA is developed with a lower incidence and severity (18, 28).

Several non excluding mechanisms may explain the exacerbation of CIA in B10.RIII.*ApoE*$^{-/-}$ mice. ApoE-containing lipoproteins are very efficient suppressing mitogen-induced proliferative responses of lymphocytes (29). In CD4^{+} and CD8^{+} T cells this effect seems to be, at least in part, dependent on the reduction in the production of biologically active IL-2 (29). Furthermore, the intravenous administration of a small ApoE-mimetic peptide derived from the receptor-binding region of the ApoE holoprotein has been shown to suppress both systemic and brain inflammatory responses in mice after lipopolysaccharide administration (30). The anti-inflammatory capacity of ApoE appears to be isoform-dependent, and in the above mentioned experimental models of brain inflammation, animals expressing the E4 allele have greater inflammatory responses (30). Interestingly, there exists an association between the ApoE4 genotype and bone loss in human RA (31). Thus, the enhanced CIA of B10.RIII.*ApoE*$^{-/-}$ mice may be directly linked with the absence of the anti-inflammatory properties of ApoE. On the other hand, the deficiency in ApoE causes important

changes in the serum lipid profile of B10.RIII.*ApoE*$^{-/-}$ mice, with a remarkable inversion in the LDL-c/HDL-c ratio in comparison to B10.RIII.WT mice. These changes may be relevant for the induction of inflammatory responses since HDL possess immunomodulatory properties by inhibiting the expression of pro- rather than anti-inflammatory molecules (32) or by its ability to protect LDL against oxidation (8-11). In humans, oxidized LDLs can be seen as an autoantigen inducing humoral immune responses that through the activation of complement may induce cytokine production by macrophages (33, 34). The absence of ApoE may also alter the protein composition of either the subclass of HDL with ApoE or the entire fraction of serum HDLs, secondary to the induction of inflammatory responses, promoting the generation of HDLs with pro-inflammatory functions. In this regard, the levels of pro-inflammatory HDLs with modified protein content have been reported to be increased in a cohort of patients with active RA (35). Experiments are in progress to explore such possibility in B10.RIII.*ApoE*$^{-/-}$ mice during CIA development.

Studies performed in animals immunologically depleted or genetically deficient in B cells underline the importance of humoral immune responses in the induction of CIA (36, 37). Strikingly, B10.RIII.*ApoE*$^{-/-}$ mice developing a more severe CIA than B10.RIII.WT mice, exhibit lower serum levels of IgG1, but not IgG2a, anti-col II antibodies. However, it should be stressed that not all antibodies produced in the course of an autoimmune reaction may be indeed pathogenic. In this regard, it has been demonstrated that the IgG2a switch variant of an anti-red blood cell autoantibody is about 20 times more pathogenic that the IgG1 switch variant (38), in clear correlation with the different affinities of IgG2a and IgG1 antibodies for Fcγ receptors promoting antibody-dependent cellular cytotoxicity (39). In addition, IgG2a antibodies activate much better the complement cascade than IgG1 antibodies (40).

Independently of the pathogenicity of IgG1 and IgG2a anti-col II antibodies in CIA development, the reduction in the levels of circulating IgG1 anti-col II antibodies observed in B10.RIII.*ApoE*$^{-/-}$ mice compared to B10.RIII.WT mice indirectly reflects a distinct pattern of functional CD4 T cell differentiation between both strains of mice after col II immunization. The increased joint expression of the Th1 cytokine IFNγ and of the Th17 cytokines IL-17 and IL-21 but not of the Th2 cytokine IL-4 or of the Treg cytokine TGFβ1, and the expansion of Th1 and Th17 cells, but not Tregs, in the draining lymph nodes observed in col II-CFA immunized B10.RIII.*ApoE*$^{-/-}$ mice, confirm this assumption. Whereas the pathogenic role of Th17 cells in the development of CIA has been clearly defined (15, 16), the contribution of Th1 cells is less clear. Thus, IFNγ deficiency renders the normally resistant B6 strain susceptible to disease (41, 42), and lack of IFNγ or signalling through the IFNγ receptor enhances the severity of arthritis in susceptible strains such as DBA/1 (43, 44). On the other hand, enhanced Th1 and Th17 immune responses are observed in experimental situations associated to exacerbated CIA, such as in mice with a deficiency of myeloid cell-specific IL-1 receptor antagonist (45). Whether the increased joint expression of IFNγ and the expansion of Th1 cells in secondary lymphoid organs play a pathogenic or regulatory activity in CIA development of B10.RIII.*ApoE*$^{-/-}$ mice remains to be determined.

One of the final consequences of the exacerbated CIA in B10.RIII.*ApoE*$^{-/-}$ mice, was the increase in the expression of multiple pro-inflammatory and arthritogenic cytokines in the joint such as IL-1β and IL-6. However, despite the enhanced CIA observed in these animals, the expression of TNFα in the joints remained similar to that of CIA-developing B10.RIII.WT mice. Although these results might appear to be paradoxical, it was described recently that TNF blockade using TNFR-Fc fusion protein or anti-TNF monoclonal antibodies unexpectedly, expanded populations of Th1 and

Th17 cells, which were shown by adoptive transfer to be pathogenic (46). Thus, an additional local increase in the expression of TNFα over the already excessive and pathogenic production of TNFα in RA (47) might have regulatory properties by limiting pathogenic $CD4^+$ T-cell responses. Alternatively, since TNFα expression can be regulated at multiple levels including post-transcriptional mechanism (48), it might be possible that the production and release of TNFα protein in B10.RIII.*ApoE*$^{-/-}$ mice developing a severe CIA was increased in the absence of an upregulation of TNFα mRNA expression in the joints.

Unlike CIA, the severity of atherosclerosis is not affected by the development of arthritis in col II-CFA immunized B10.RIII.*ApoE*$^{-/-}$ mice. Thus, the extent of vascular lesions in these col II-CFA immunized mice is similar to that of PBS-CFA immunized controls. In addition, a similar content of macrophages is observed in the atherosclerotic lesions of PBS-CFA treated and col II-CFA immunized B10.RIII.*ApoE*$^{-/-}$mice, indicating that the lack of enhanced vascular lesions in col II-CFA immunized B10.RIII.*ApoE*$^{-/-}$mice is not related to a preferential migration of inflammatory cells to the affected joints instead of the vessels. However, it should be noted that adjuvants, including CFA, possess a potent atheroprotective capacity (25) that can mask the potential pro-atherogenic effect associated to the systemic inflammatory environment found in the arthritis-developing animals. In agreement with this possibility and with previous reports (25), we have observed that the extent of atherosclerosis at the level of the aortic sinus in untreated B10.RIII.*ApoE*$^{-/-}$ mice is significantly higher than that of B10.RIII.*ApoE*$^{-/-}$ mice immunized with PBS-CFA, which fail to develop CIA (data not shown). This observation clearly indicates that an experimental model of RA requiring the use of CFA for its induction is not appropriated to study cellular and molecular

mechanisms responsible for the accelerated atherosclerosis associated to this systemic autoimmune disease.

In conclusion, we provide evidences about how a metabolic abnormality associated with dyslipidemia (ApoE deficiency) may influence the development of an autoimmune disease such as RA that can be useful for the design of new therapeutic strategies in humans.

ACKNOWLEDGEMENTS

We thank Drs Marcos López-Hoyos and Miguel Angel González-Gay, Hospital Universitario Marqués de Valdecilla, Santander and Dr Jaime Calvo, Hospital Sierrallana, Torrelavega, Spain for comments to the manuscript and to Maria Aramburu, Natalia Cobo and Iván Gómez for technical assistance. The authors have no conflicting financial interests.

AUTHOR CONTRIBUTIONS

All authors were involved in drafting the article or revising it critically for important intellectual content, and all authors approved the final version to be published. Dr. R. Merino had full access to all of the data in the study and takes responsibility for the integrity of the data and the accuracy of the data analysis.

Study conception and design. Postigo, Rodríguez-Rey, J. Merino, R. Merino.

Acquisition of data. Postigo, Genre, Iglesias, Fernández-Rey, Buelta.

Analysis and interpretation of data. Postigo, Rodríguez-Rey, J. Merino, R. Merino.

REFERENCES

1. Gonzalez-Gay MA, Gonzalez-Juanatey C, Martin J. Rheumatoid arthritis: a disease associated with accelerated atherogenesis. Semin Arthritis Rheum 2005;35:8–17.
2. Young A, Koduri G, Batley M, Kulinskaya E, Gough A, Norton S, et al. Mortality in rheumatoid arthritis. Increased in the early course of disease, in ischaemic heart disease and in pulmonary fibrosis. Rheumatology (Oxford) 2007;46:350-7.
3. del Rincon ID, Williams K, Stern MP, Freeman GL, Escalante A. High incidence of cardiovascular events in a rheumatoid arthritis cohort not explained by traditional cardiac risk factors. Arthritis Rheum 2001;44:2737-45.
4. Choi HK, Seeger JD. Lipid profiles among US elderly with untreated rheumatoid arthritis--the Third National Health and Nutrition Examination Survey. J Rheumatol 2005;32:2311–6.
5. Park YB, Lee SK, Lee WK, Suh CH, Lee CW, Lee CH, et al. Lipid profiles in untreated patients with rheumatoid arthritis. J Rheumatol 1999;26:1701–4.
6. Yoo WH. Dyslipoproteinemia in patients with active rheumatoid arthritis: effects of disease activity, sex, and menopausal status on lipid profiles. J Rheumatol 2004;31:1746–53.
7. van Halm VP, Nielen MM, Nurmohamed MT, van Schaardenburg D, Reesink HW, Voskuyl AE, et al. Lipids and inflammation: serial measurements of the lipid profile of blood donors who later developed rheumatoid arthritis. Ann Rheum Dis 2007;66:184–8.
8. Mahley RW. Apolipoprotein E: cholesterol transport protein with expanding role in cell biology. Science 1988;240:622–30.

9. Hui DY, Harmony JAK, Innerarity TL, Mahley RW. Immunoregulatory plasma lipoproteins. Role of apoprotein E and apoprotein B. J Biol Chem 1980;255:11775–81.
10. Navab M, Hama SY, Cooke CJ, Anantharamaiah GM, Chaddha M, Jin L, et al. Normal high density lipoprotein inhibits three steps in the formation of mildly oxidized low density lipoprotein: step 1. J Lipid Res 2000;41:1481–94.
11. Navab M, Hama SY, Anantharamaiah GM, Hassan K, Hough GP, Watson AD, et al. Normal high density lipoprotein inhibits three steps in the formation of mildly oxidized low density lipoprotein: steps 2 and 3. J Lipid Res 2000;41:1495–508.
12. Daugherty A. Mouse models of atherosclerosis. Am J Med Sci 2002;323:3-10.
13. Fazio S, Linton MF. Mouse models of hyperlipidemia and atherosclerosis. Front Biosci 2001;6:D515-25.
14. Gustafsson K, Karlsson M, Andersson L, Holmdahl R. Structures on the I-A molecule predisposing for susceptibility to type II collagen-induced autoimmune arthritis. Eur J Immunol 1990;20:2127-31.
15. Xie JJ, Wang J, Tang TT, Chen J, Gao XL, Yuan J, et al. The Th17/Treg functional imbalance during atherogenesis in ApoE(-/-) mice. Cytokine 2010;49:185-93.
16. Smith E, Prasad KM, Butcher M, Dobrian A, Kolls JK, Ley K, et al. Blockade of interleukin-17A results in reduced atherosclerosis in apolipoprotein E-deficient mice. Circulation 2010;121:1746-55.
17. Lubberts E, Koenders MI, Oppers-Walgreen B, Bersselaar L van den, Coenen-de Roo CJ, Joosten LA, et al. Treatment with a neutralizing anti-murine interleukin-17 antibody after the onset of collagen-induced arthritis reduces joint

Arthritis Rheum 2004;50:650–659.

18. Sato K, Suematsu A, Okamoto K, Yamaguchi A, Morishita Y, Kadono Y, et al. Th17 functions as an osteoclastogenic helper T cell subset that links T cell activation and bone destruction. J Exp Med 2006;203:2673–82.

19. Littman DR, Rudensky AY. Th17 and regulatory T cells in mediating and restraining inflammation. Cell 2010;140:845-58.

20. Asquith DL, Miller AM, Hueber AJ, Liew FY, Sattar N, McInnes IB. Apolipoprotein E-deficient mice are resistant to the development of collagen-induced arthritis. Arthritis Rheum 2010;62:472-7.

21. González J, Tamayo E, Santiuste I, Marquina R, Buelta L, González-Gay MA, et al. $CD4^{+}CD25^{+}$ T cell-dependent inhibition of autoimmunity in transgenic mice overexpressing human Bcl-2 in T lymphocytes. J Immunol 2007;178:2778–86.

22. Sancho D, Gomez M, Viedma F, Esplugues E, Gordon-Alonso M, Garcia-Lopez MA, et al. CD69 downregulates autoimmune reactivity through active transforming growth factor-β production in collagen-induced arthritis. J Clin Invest 2003;112:872–82.

23. López-Hoyos M, Marquina R, Tamayo E, González-Rojas J, Izui S, Merino R, et al. Defects in the regulation of B cell apoptosis are required for the production of citrullinated peptide autoantibodies in mice. Arthritis Rheum 2003;48:2353-61.

24. Marquina R, Díez MA, López-Hoyos M, Buelta L, Kuroki A, Kikuchi S, et al. Inhibition of B cell death causes the development of an IgA nephropathy in (New Zealand white x C57BL/6)F(1)-bcl-2 transgenic mice. J Immunol 2004;172:7177-85.

25. Khallou-Laschet J, Tupin E, Caligiuri G, Poirier B, Thieblemont N, Gaston AT, et al. Atheroprotective effect of adjuvants in apolipoprotein E knockout mice. Atherosclerosis 2006;184:330-41.

26. González-Navarro H, Abu Nabah YN, Vinué A, Andrés-Manzano MJ, Collado M, Serrano M, et al. p19(ARF) deficiency reduces macrophage and vascular smooth muscle cell apoptosis and aggravates atherosclerosis. J Am Coll Cardiol 2010;55:2258-68.

27. Cho YG, Cho ML, Min SY, Kim HY. Type II collagen autoimmunity in a mouse model of human rheumatoid arthritis. Autoimmun Rev 2007;7:65-70.

28. Campbell IK, Hamilton JA, Wicks IP. Collagen-induced arthritis in C57BL/6 (H-2^b) mice: new insights into an important disease model of rheumatoid arthritis. Eur J Immunol 2000;30:1568–75.

29. Kelly ME, Clay MA, Mistry MJ, Hsieh-Li H-M, Harmony JAK. Apolipoprotein E inhibition of proliferation of mitogen-activated T lymphocytes: production of interleukin 2 with reduced biological activity. Cell Immunol 1994;159:124–39.

30. Lynch JR, Tang W, Wang H, Vitek MP, Bennett ER, Sullivan PM, et al. APOE genotype and an ApoE-mimetic peptide modify the systemic and central nervous system inflammatory response. J Biol Chem 2003;278:48529-33.

31. Lee SI, Lee SY, Yoo WH. Association of apolipoprotein E polymorphism with bone mineral density in postmenopausal women with rheumatoid arthritis. Rheumatology (Oxford) 2005;44:1067-8.

32. Gruaz L, Delucinge-Vivier C, Descombes P, Dayer JM, Burger D. Blockade of T cell contact-activation of human monocytes by high-density lipoproteins reveals a new pattern of cytokine and inflammatory genes. PLoS ONE 2010;5:e9418.

33. Saad AF, Virella G, Chassereau C, Boackle RJ, Lopes-Virella MF. OxLDL immune complexes activate complement and induce cytokine production by MonoMac 6 cells and human macrophages. J Lipid Res 2006;47:1975-83.

34. Lopes-Virella MF, Virella G. Clinical significance of the humoral immune response to modified LDL. Clin Immunol 2010;134:55-65.

35. Charles-Schoeman C, Watanabe J, Lee YY, Furst DE, Amjadi S, Elashoff D, et al. Abnormal function of high-density lipoprotein is associated with poor disease control and an altered protein cargo in rheumatoid arthritis. Arthritis Rheum 2009;60:2870-9.

36. Yanaba K, Hamaguchi Y, Venturi GM, Steeber DA, St Clair EW, Tedder TF. B cell depletion delays collagen-induced arthritis in mice: arthritis induction requires synergy between humoral and cell-mediated immunity. J Immunol 2007;179:1369-80.

37. Svensson L, Jirholt J, Holmdahl R, Jansson L. B cell-deficient mice do not develop type II collagen-induced arthritis (CIA). Clin Exp Immunol 1998;111:521-6.

38. Fossati-Jimack L, Ioan-Facsinay A, Reininger L, Chicheportiche Y, Watanabe N, Saito T, et al. Markedly different pathogenicity of four immunoglobulin G isotype-switch variants of an antierythrocyte autoantibody is based on their capacity to interact in vivo with the low-affinity Fcγ receptor III. J Exp Med 2000;191:1293-302.

39. Ravetch JV, Bolland S. IgG Fc receptors. Annu Rev Immunol 2001;19:275-90.

40. Neuberger MS, Rajewsky K. Activation mouse complement by monoclonal mouse antibodies. Eur J Immunol 1981;11:1012-16.

41. Chu CQ, Song Z, Mayton L, Wu B, Wooley PH. IFNγ deficient C57BL/6 (H-2b) mice develop collagen induced arthritis with predominant usage of T cell receptor Vβ6 and Vβ8 in arthritic joints. Ann Rheum Dis 2003;62:983–90.

42. Guedez YB, Whittington KB, Clayton JL, Joosten LA, van de Loo FA, van den Berg WB, et al. Genetic ablation of interferon-γ up-regulates interleukin-1α expression and enables the elicitation of collagen-induced arthritis in a nonsusceptible mouse strain. Arthritis Rheum 2001;44:2413–24.

43. Manoury-Schwartz B, Chiocchia G, Bessis N, Abehsira-Amar O, Batteux F, Muller S, et al. High susceptibility to collagen-induced arthritis in mice lacking IFN-γ receptors. J Immunol 1997;158: 5501–6.

44. Vermeire K, Heremans H, van de Putte M, Huang S, Billiau A, Matthys P. Accelerated collagen-induced arthritis in IFN-γ receptor-deficient mice. J Immunol 1997;158:5507–13.

45. Lamacchia C, Palmer G, Seemayer CA, Talabot-Ayer D, Gabay C. Enhanced Th1 and Th17 responses and arthritis severity in mice with a deficiency of myeloid cell-specific interleukin-1 receptor antagonist. Arthritis Rheum 2010;62:452-62.

46. Notley CA, Inglis JJ, Alzabin S, McCann FE, McNamee KE, Williams RO. Blockade of tumor necrosis factor in collagen-induced arthritis reveals a novel immunoregulatory pathway for Th1 and Th17 cells J Exp Med 2008;205:2491-7.

47. Elliott MJ, Maini RN, Feldmann M, Kalden JR, Antoni C, Smollen JS, et al. Treatment with a chimaeric monoclonal antibody to tumour necrosis factor α suppresses disease activity in rheumatoid arthritis: results of a multi-centre, randomised, double blind trial. Lancet 1994;344:1105–10.

48. Schottelius AJ, Moldawer LL, Dinarello CA, Asadullah K, Sterry W, Edwards CK 3rd. Biology of tumor necrosis factor-alpha- implications for psoriasis. Exp Dermatol 2004;13:193-222.

FIGURE LEGENDS

Figure 1: Serum lipid profiles in B10.RIII.*ApoE*$^{-/-}$ mice during CIA development. (A) Levels of total cholesterol, HDLc and VLDL/LDLc and (B) levels of triglycerides were determined in the sera of B10.RIII.WT and B10.RIII.*ApoE*$^{-/-}$ male mice 8 weeks after induction of CIA. Representative results of 3 independent experiments are expressed as the mean ± SD (8-10 animals/group). Statistic differences between B10.RIII.WT and B10.RIII.*ApoE*$^{-/-}$ mice are indicated as follow: ***p<0.001. For both A and B, the lowest limits of detection were 0.5 mg/dl.

Figure 2: Exacerbated clinical signs and altered anti-col II antibody responses in CIA developing B10.RIII.*ApoE*$^{-/-}$ mice. 8-12 weeks-old B10.RIII.WT and B10.RIII.*ApoE*$^{-/-}$ male mice were immunized with col II-CFA. (A) Cumulative incidence of CIA. Results are expressed as the mean ± SD of the percentage of affected mice at the indicated weeks after immunization (n= 26 mice/group). (B) Clinical severity of CIA 8 weeks after immunization with col II-CFA. (C) Serum levels of IgG1 and IgG2a anti-col II antibodies before and 8 weeks after immunization with col II-CFA. In B and C values of individual mice are expressed. Bars represent the mean value of each examination. Statistic differences between B10.RIII.WT and B10.RIII.*ApoE*$^{-/-}$ mice are indicated as follow: *p<0.05, **p<0.01.

Figure 3: Exacerbated radiological and histopathological lesions in B10.RIII.*ApoE*$^{-/-}$ mice during CIA development. 8-12 weeks-old B10.RIII.WT and B10.RIII.*ApoE*$^{-/-}$ male mice were immunized with col II-CFA. (A) Representative radiological images of the front paws of B10.RIII.WT and B10.RIII.*ApoE*$^{-/-}$ mice non-immunized (Non-I) and 8 weeks after immunization with col II-CFA (Col II-I). (B) Radiological score of four

individual signs expressed as the mean ± SD from three independent experiments (20-25 animals/group). (C) Representative histological appearance of the joints (x10) of B10.RIII.WT and B10.RIII.*ApoE*$^{-/-}$ mice non-immunized and 8 weeks after immunization with col II-CFA. (D) Histological score of the joints 8 weeks after immunization with col II-CFA expressed as the mean ± SD of the percentage of joints ascribed to each severity group from three independent experiments (20-25 animals/group). In B and D statistic differences between B10.RIII.WT and B10.RIII.*ApoE*$^{-/-}$ mice are indicated as follow: *p<0.05, **p<0.01, *** p<0.005.

Figure 4: Increased expression of pro-inflammatory citokines in the joints of B10.RIII.*ApoE*$^{-/-}$ mice during CIA development. Analysis by quantitative real-time RT-PCR of mRNA from different cytokines in the paws of B10.RIII.WT and B10.RIII.*ApoE*$^{-/-}$ mice, non-immunized (open bars) and 8 weeks after immunization with col II-CFA (closed bars). Results from three independent experiments (15-20 animals/group) are expressed as mean ± SD fold change of each cytokine relative to GAPDH expression measured in parallel in each sample. Statistic differences are indicated as follow: *p<0.05, **p<0.01, *** p<0.005.

Figure 5: Expansion of Th1 and Th17 but not Treg cells in the draining lymph nodes of col II-immunized B10.RIII.*ApoE*$^{-/-}$ mice. 8-12 weeks-old B10.RIII.WT and B10.RIII.*ApoE*$^{-/-}$ male mice were immunized with col II-CFA. For intracellular cytokine staining, lymphocytes from paraaortic lymph nodes were stimulated 3 weeks after immunization with phorbol myristate acetate and ionomycin in the presence of GolgiStop solution. (A) Representative histograms of $CD4^+IFN\gamma^+$ Th1, $CD4^+IL\text{-}17^+$ Th17 and $CD4^+CD25^+FoxP3^+$ Treg cells, determined by flow cytometry, in the different experimental groups. The percentage of each population is indicated. (B) Percentages of

$CD4^+IFN\gamma^+$ Th1 (left panel), $CD4^+IL\text{-}17^+$ Th17 (middle panel) and $CD4^+CD25^+FoxP3^+$ Treg (right panel) cells in non-immunized (open symbols) and 3 weeks post-immunized (closed symbols) mice. Values of individual mice are expressed. Bars represent the mean value of each examination. Statistic differences are indicated as follow: ns: non significant, **p<0.01. No differences in the number of total lymph node cells were observed within each group (non-immunized or col II-immunized) between B10.RIII.WT and B10.RIII.*ApoE*$^{-/-}$ mice.

Figure 6: Lack of exacerbation of atherosclerosis by CIA in B10.RIII.*ApoE*$^{-/-}$ mice. (A) Representative histological aspect of the aortic sinus stained with hematoxylin and eosin (upper panels, x10) and content of Mac2-immunoreactive macrophages in the atherosclerotic lesions (lower panels, x20) of age-matched non-treated B10.RIII.WT mice, 8 weeks PBS-CFA post-immunized B10.RIII.*ApoE*$^{-/-}$ mice and 8 weeks col II-CFA post-immunized B10.RIII.*ApoE*$^{-/-}$ mice. (B) Percentages of the affected area, determined by computer-assisted morphometry, from two independent experiments in the different experimental groups. Values of individual mice are expressed. Bars represent the mean value of each examination. (C) Lesion content of macrophages determined by immunohistochemistry using an anti-Mac2 mAb. Representative results of 2 independent experiments are expressed as the mean ± SD (5 animals/group) of the percentages of stained area relative to the area occupied by atheroma.

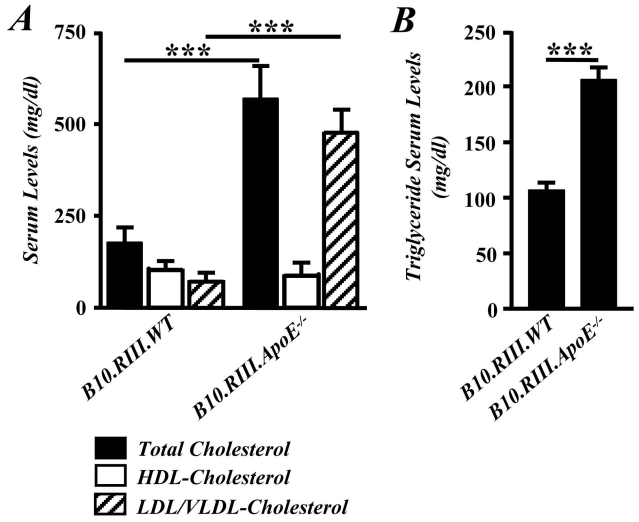

Figure 1: Serum lipid profiles in B10.RIII.*ApoE*$^{-/-}$ mice during CIA development. A) Levels of total cholesterol, HDLc and VLDL/LDLc and B) levels of triglycerides were determined in the sera of B10.RIII.WT and B10.RIII.*ApoE*$^{-/-}$ male mice 8 weeks after induction of CIA. Representative results of 3 independent experiments are expressed as the mean ± SD (8-10 animals/group). Statistic differences between B10.RIII.WT and B10.RIII.*ApoE*$^{-/-}$ mice are indicated as follow: ***p<0.001. For both A and B, the lowest limits of detection were 0.5 mg/dl.

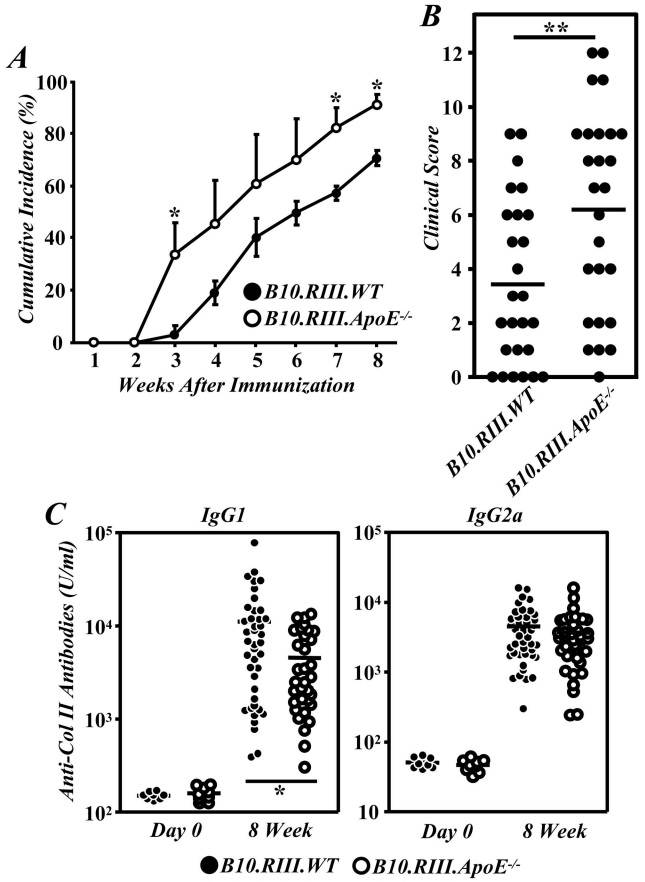

Figure 2: Exacerbated clinical signs and altered anti-col II antibody responses in CIA developing B10.RIII.*ApoE*$^{-/-}$ mice. 8-12 weeks-old B10.RIII.WT and B10.RIII.*ApoE*$^{-/-}$ male mice were immunized with col II-CFA. A) Cumulative incidence of CIA. Results are expressed as the mean ± SD of the percentage of affected mice at the indicated weeks after immunization (n= 26 mice/group). B) Clinical severity of CIA 8 weeks after immunization with col II-CFA. C) Serum levels of IgG1 and IgG2a anti-col II antibodies before and 8 weeks after immunization with col II-CFA. In B and C values of individual mice are expressed. Bars represent the mean value of each examination. Statistic differences between B10.RIII.WT and B10.RIII.*ApoE*$^{-/-}$ mice are indicated as follow: *$p<0.05$, **$p<0.01$.

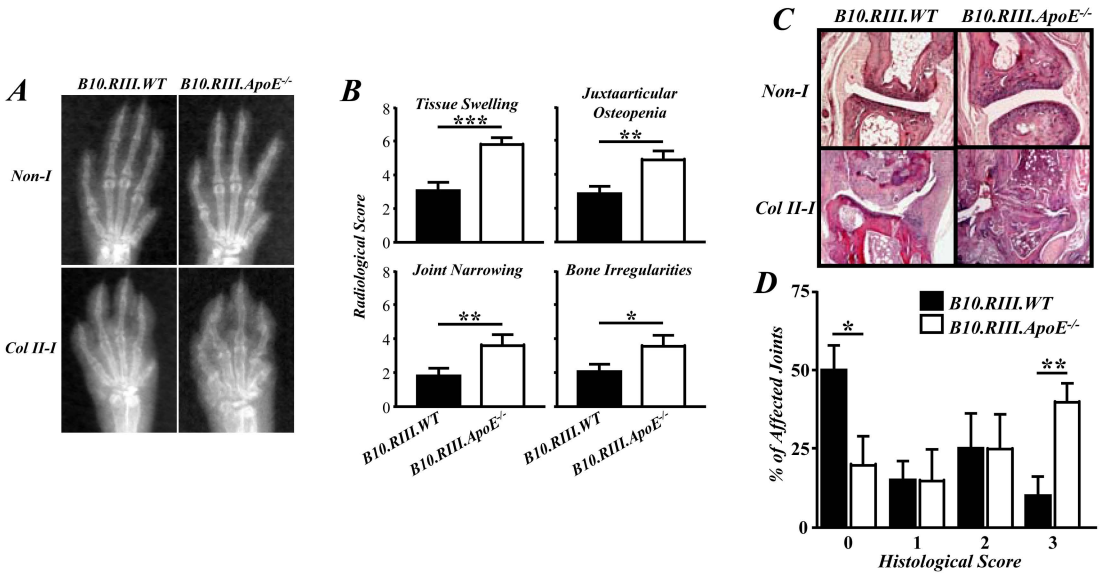

Figure 3: Exacerbated radiological and histopathological lesions in B10.RIII.*ApoE*$^{-/-}$ mice during CIA development. 8-12 weeks-old B10.RIII.WT and B10.RIII.*ApoE*$^{-/-}$ male mice were immunized with col II-CFA. A) Representative radiological images of the front paws of B10.RIII.WT and B10.RIII.*ApoE*$^{-/-}$ mice non-immunized (Non-I) and 8 weeks after immunization with col II-CFA (Col II-I). B) Radiological score of four individual signs expressed as the mean ± SD from three independent experiments (20-25 animals/group). (C) Representative histological appearance of the joints (x10) of B10.RIII.WT and B10.RIII.*ApoE*$^{-/-}$ mice non-immunized and 8 weeks after immunization with col II-CFA. D) Histological score of the joints 8 weeks after immunization with col II-CFA expressed as the mean ± SD of the percentage of joints ascribed to each severity group from three independent experiments (20-25 animals/group). In B and D statistic differences between B10.RIII.WT and B10.RIII.*ApoE*$^{-/-}$ mice are indicated as follow: *p<0.05, **p<0.01, *** p<0.005.

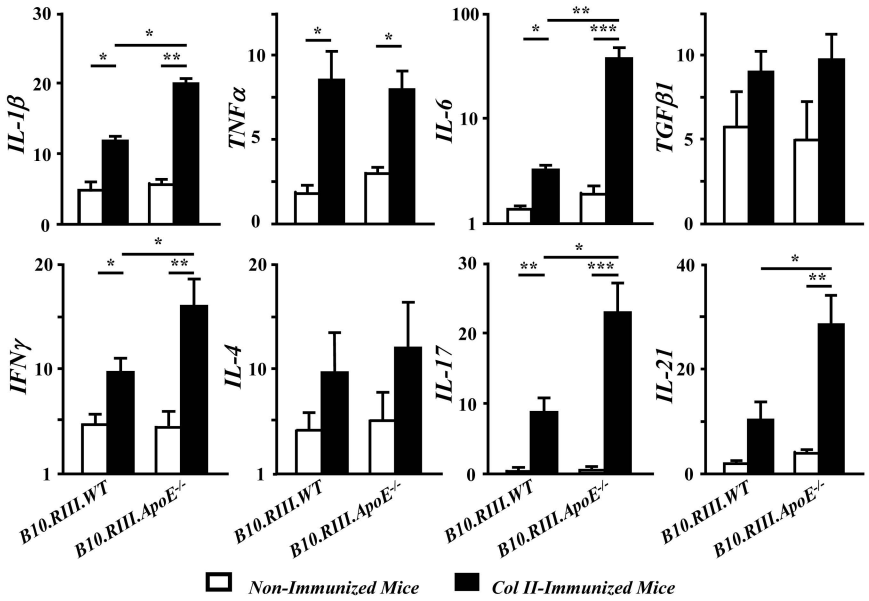

Figure 4: Increased expression of pro-inflammatory citokines in the joints of B10.RIII.*ApoE*-/- mice during CIA development. Analysis by quantitative real-time RT-PCR of mRNA from different cytokines in the paws of B10.RIII.WT and B10.RIII.*ApoE*-/- mice, non-immunized (open bars) and 8 weeks after immunization with col II-CFA (closed bars). Results from three independent experiments (15-20 animals/group) are expressed as mean ± SD fold change of each cytokine relative to GAPDH expression measured in parallel in each sample. Statistic differences are indicated as follow: *p<0.05, **p<0.01, *** p<0.005.

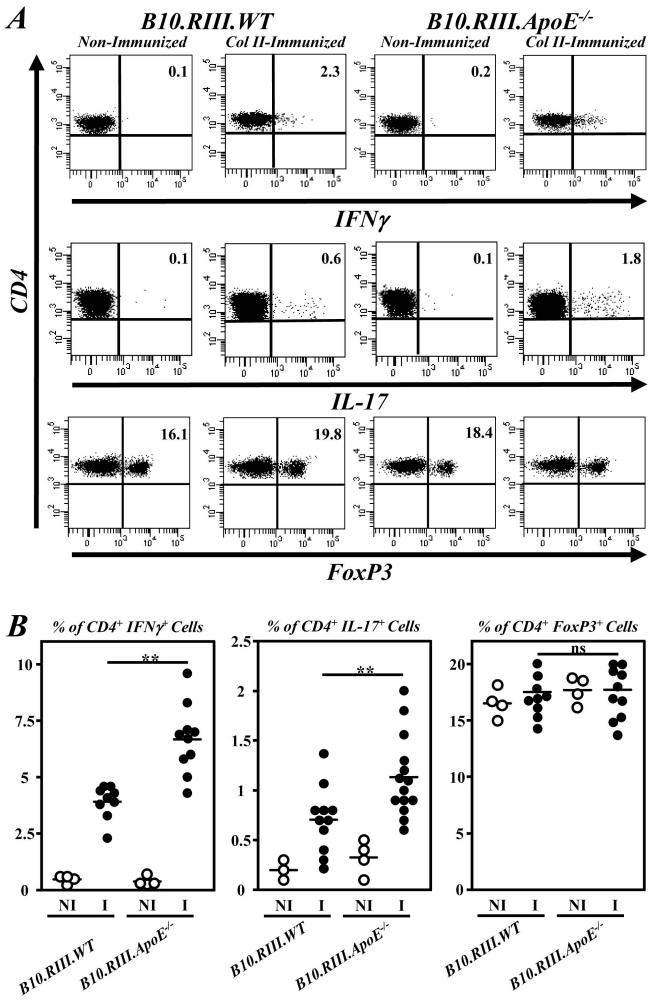

Figure 5: Expansion of Th1 and Th17 but not Treg cells in the draining lymph nodes of col II-immunized B10.RIII.*ApoE*$^{-/-}$ mice. 8-12 weeks-old B10.RIII.WT and B10.RIII.*ApoE*$^{-/-}$ male mice were immunized with col II-CFA. For intracellular cytokine staining, lymphocytes from paraaortic lymph nodes were stimulated 3 weeks after immunization with phorbol myristate acetate and ionomycin in the presence of GolgiStop solution. (A) Representative histograms of $CD4^+IFN\gamma^+$ Th1, $CD4^+IL\text{-}17^+$ Th17 and $CD4^+CD25^+FoxP3^+$ Treg cells, determined by flow cytometry, in the different experimental groups. The percentage of each population is indicated. (B) Percentages of $CD4^+IFN\gamma^+$ Th1 (left panel), $CD4^+IL\text{-}17^+$ Th17 (middle panel) and $CD4^+CD25^+FoxP3^+$ Treg (right panel) cells in non-immunized (open symbols) and 3 weeks post-immunized (closed symbols) mice. Values of individual mice are expressed. Bars represent the mean value of each examination. Statistic differences are indicated as follow: ns: non significant, **p<0.01. No differences in the number of total lymph node cells were observed within each group (non-immunized or col II-immunized) between B10.RIII.WT and B10.RIII.*ApoE*$^{-/-}$ mice.

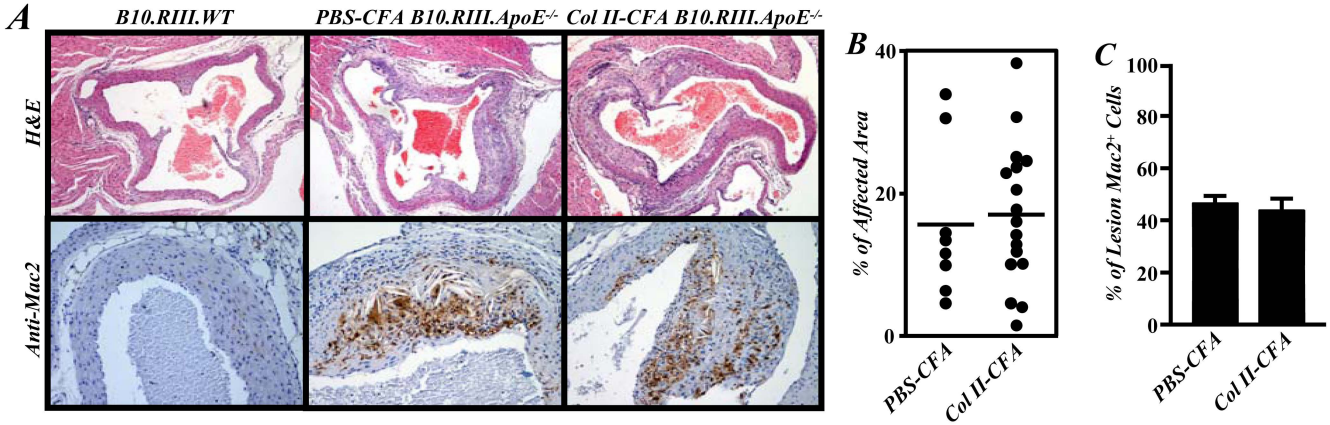

Figure 6: Lack of exacerbation of atherosclerosis by CIA in B10.RIII.*ApoE*$^{-/-}$ mice. (A) Representative histological aspect of the aortic sinus stained with hematoxylin and eosin (upper panels, x10) and content of Mac2-immunoreactive macrophages in the atherosclerotic lesions (lower panels, x20) of age-matched non-treated B10.RIII.WT mice, 8 weeks PBS-CFA post-immunized B10.RIII.*ApoE*$^{-/-}$ mice and 8 weeks col II-CFA post-immunized B10.RIII.*ApoE*$^{-/-}$ mice. (B) Percentages of the affected area, determined by computer-assisted morphometry, from two independent experiments in the different experimental groups. Values of individual mice are expressed. Bars represent the mean value of each examination. (C) Lesion content of macrophages determined by immunohistochemistry using an anti-Mac2 mAb. Representative results of 2 independent experiments are expressed as the mean ± SD (5 animals/group) of the percentages of stained area relative to the area occupied by atheroma.